Multi-Mode Narrow-Frame Antenna for 4G/5G Metal-Rimmed Mobile Phones

M. Yang [1,2], Y. F. Sun [1*], and T. Q. Liao [1]

[1] Key Lab of Intelligent Computing and Signal Processing, Ministry of Education
Anhui University, Hefei 230601, China
myang@ahu.edu.cn, *yfsun_ahu@sina.com, t.liao@ahu.edu.cn

[2] Electronics and Information Engineering Department
Bozhou University, Bozhou 236800, China

Abstract ─ A novel multi-mode narrow-frame antenna is presented for 4G/5G metal-rimmed mobile phones in this paper. The proposed antenna is constituted by a monopole antenna and a coupling strip, which is printed on FR4 substrate with thickness of 0.8 mm. The overall area occupied by the antenna is only 60×10.4 mm^2, which can be used as a promising narrow-frame antenna. The simulated results shows that the return loss of the antenna can provide four operating bandwidths of 822–961 (band 1), 1697–3075 (band 2), 3280–3835 (band 3) and 4475–5050 MHz (band 4), which respectively cover 824–960, 1710–2690, 3300–3600 and 4800–5000 MHz in 4G/5G communication systems. In order to verify the accuracy of theoretical analysis and simulated results, the proposed antenna is fabricated and measured. The experimental results are basically consistent with the simulated results, suggesting that the presented antenna has attractive performance for mobile phones.

Index Terms ─ Frame antenna, metal rim, multi-mode, nona-band operation.

I. INTRODUCTION

As the radio access technologies develop rapidly, an increasing number of portable devices can support the LTE function [1–2], especially metal-framed smartphones have evolved into fashionable and popular products for consumers [3–4]. Nevertheless, the metal characteristics of the bezel of the smartphone affect the internal antenna's performance to a certain extent. Recently, designing the metal frame of a mobile phone with a novel structure has become the key to solving the problem. In [5–6], grounded patches and gaps are utilized to compensate for the performance loss due to the antenna being mounted internally. A novel method which takes part or the whole of the metal rim as antenna elements is proposed in [7–9] to simplify the antenna design. Although these antennas based on metal rim have been successfully implemented, none of them cover the entire 4G/5G frequency bands.

The 5G operating license of domestic mobile phones was promulgated and thLe band division of a new generation of mobile communication was defined by China's Ministry of Industry and Information Technology in November 2017 [10]. The 3300–3600 MHz and 4800–5000 MHz bands are set as 5G wireless communication frequency bands. At the same time, some innovative 5G technologies are also proposed in other countries to obtain faster transmission rates [11-12]. Therefore, the antenna with high-performance and narrow-frame can be applied to 5G wireless communications.

In recent years, a variety of methods are employed to design antenna for 4G/5G mobile phones. On the basis of loop antenna structure, the frame antennas are designed in [13–17], but amounts of inductors and capacitors are used which markedly increase these antennas' complexity. In [18], a dual-band eight-antenna array is proposed for multiple input and multiple output (MIMO) applications in 5G mobile terminals. But, it cannot fully satisfy the requirement of 4G/5G multiband communications. In [19], a hybrid antenna is designed for 4G/5G MIMO application, which is made up of two antenna modules, namely 4G and 5G antenna modules. However, it is difficult for such a hybrid antenna to miniaturize a mobile phone antenna. Four MIMO antennas are also designed in [20-23], and the metamaterial structures are introduced to reduce the coupling between the antenna element, but the decoupling structures are not conducive to the low profile and miniaturization of the antenna.

In this paper, the characteristics of multi-mode, ultra-wideband and multi-band are integrated into an antenna which applied in the 4G/5G fields. Furthermore, the designed antenna has compact structure without any lumped elements. The wider bandwidth is also easily achieved by using an I-shaped feeding strip and a stereoscopic coupled grounding strip, which are printed on the back side of the substrate as a part of mobile phone

Submitted On: March 6, 2020
Accepted On: May 24, 2020
https://doi.org/10.47037/2020.ACES.J.350809

shells.

II. STRUCTURE AND DESIGN OF THE PROPOSED ANTENNA

2.1. Structure of Antenna

The complete geometry of the proposed antenna is shown in Fig. 1. As plotted in Fig. 1 (a), a 0.8 mm thick FR4 substrate which has a relative permittivity of 4.4 and a loss tangent of 0.02 is utilized as the mobile phone housing. The housing has a volume of 120 × 60 × 5 mm^3, and a ground plane with the size of 109.6 × 60 mm^2 is printed on the housing. A 50 Ω mini coaxial line which is connected to the feeding point (Point A) and the PCB grounding point (Point C), is employed to excite the antenna.

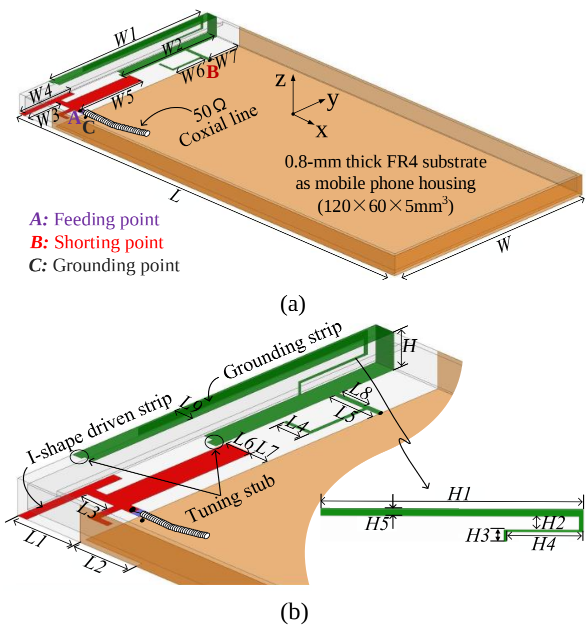

Fig. 1. (a) Configuration of proposed antenna. (b) Detail dimensions of the antenna modules (Unit: mm).

As can be seen in Fig. 1 (a), the three-branch coupled parasitic ground strip (including a long branch and two short branches) and several tuning stubs are used to excite the multiple modes which work at band 1 and band 2. The two bands can cover the 824 – 960 MHz and 1710 – 2690 MHz bands effectively. That shown in Fig. 1 (b) is the proposed antenna with detailed dimensions. In addition, the I-shape driven strip and a rectangular slot are used to excite the multiple modes which work at band 3 and band 4. The two bands can cover the 3300–3600 MHz and 4800–5000 MHz bands effectively. The working mechanism of the proposed antenna is analyzed in detail in the section 2.2.

2.2 Antenna Design and Analysis

A. Slotted loading method for the high band

In this section, the S_{11} and the evolution processes for different antennas are investigated to clearly explain the operating mechanism and design procedure of the proposed antenna. As illustrated in Fig. 2 (a), a ground clearance of 60 × 10.4 mm^2 is reserved for the band 3 and band 4. An I-shape strip (Ant1) is introduced as the monopole antenna. As shown in Fig. 2 (c), Ant1 creates two 0.25λ resonant modes respectively around 3500 MHz and 2100 MHz. The rectangular slot with 1 mm width is inserted between points *D* and *E* (Ant2) to widen the bandwidth of band 3 and band 4, which improves the impedance matching through capacity coupling and creates a 0.25λ resonant mode at around 4850 MHz.

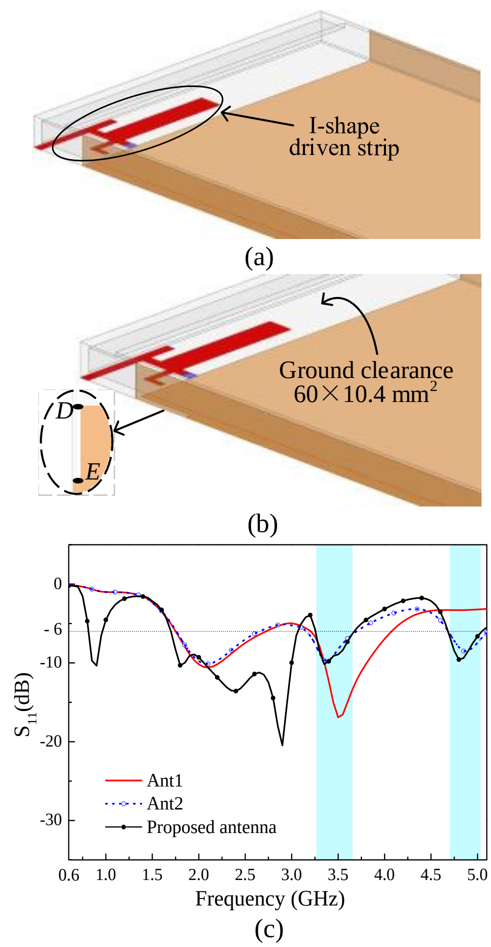

Fig. 2. Comparison of Ant1, Ant2 and simulated S_{11}. (a) Ant1, (b) Ant2, and (c) Simulated S_{11}.

For Ant2, bandwidths of 14.6% (3180–3680 MHz) and 8.6% (4680–5100 MHz) are obtained, which can meet the requirements for 5G mobile phones.

B. Technologies for the low band

According to the above analysis in section 2.2A, Ant2 can cover 3300–3600 MHz and 4800–5000 MHz. This antenna cannot cover 824–960 MHz and 1710–2690 MHz from Fig. 2 (c). An effective solution is introduced to merge multiple modes through utilizing multiple strips. Here, we will introduce the evolution process in order to cover the low band. In Figs. 3 (a)–(c), there are three types of configuration, which represent three important states during the evolution. The corresponding simulated S_{11} is also given in Fig. 3 (d).

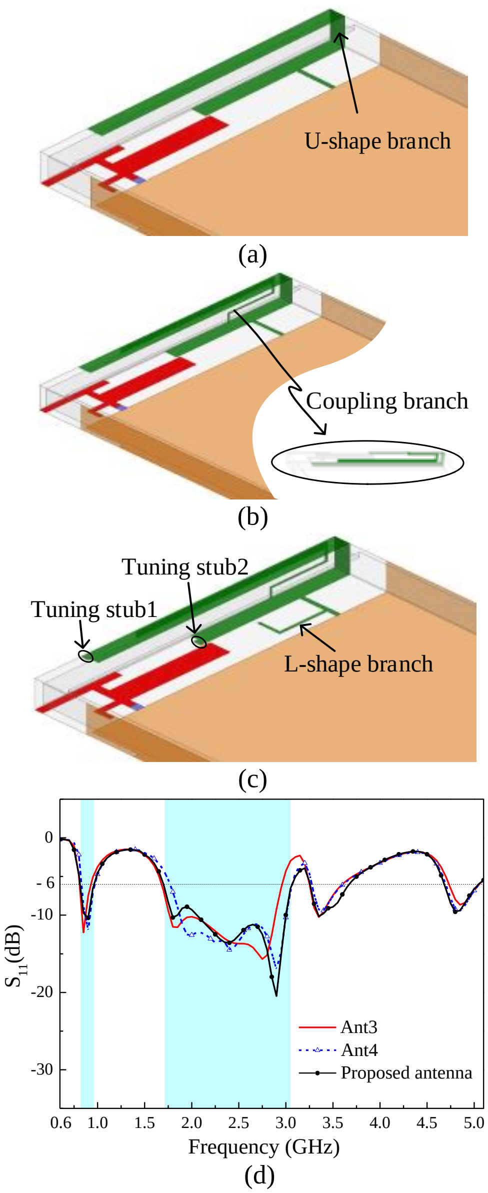

Fig. 3. Comparison of An3, Ant4, proposed antenna and simulated S_{11}: (a) Ant3, (b) Ant4, (c) the proposed antenna, and (d) simulated S_{11}.

As shown in Fig. 3 (a), a U-shape branch is inserted into Ant2 to form Ant3. The U-shape branch is disposed on the right side of the system ground plane, the length of which is 84.1 mm. Ant3 creates a 0.25λ resonant mode at around 850 MHz. In order to broaden the bandwidth of the band 1, a coupling branch is added to Ant3 to form Ant4, as shown in Fig. 3 (b). Thus, the resonance point at 850 MHz is shifted to 900 MHz, and its bandwidth is 820–973 MHz. To obtain a characteristic of broadband which coverage in the 1710 MHz frequency band, an L-shape branch and two tuning stubs are inserted into Ant4 to form the proposed antenna. As illustrated in Fig. 3 (d), by inserting the L-shape branch and two tuning stubs, the band 2 is enhanced. The simulated results show that the S_{11} of the frequency band 1700–3061 MHz is less than -6 dB. So, the proposed antenna can cover LTE/WWAN (4G) bands.

The antenna configuration is modeled by HFSS full-wave simulator and optimized design parameters are listed in Table 1.

Table 1: Geometric parameters of the proposed antenna (Unit: mm)

Parameter	Value	Parameter	Value
W	60.0	H_1	38.4
L	120.0	H_2	2.0
H	5.0	H_3	1.8
W_1	50.8	W_5	20.2
W_2	29.8	W_6	9.5
W_3	10.0	W_7	9.2
L_1	10.4	L_6	4.0
L_2	9.4	L_7	3.0
L_3	4.7	H_4	11.2
W_4	16.0	H_5	1.0
L_4	4.5	L_8	5.0
L_5	7.4	L_9	3.0

C. Operating principle

The surface current distributions of the proposed antenna at 900, 1800, 2400, 3350 and 4800 MHz are simulated as depicted in Figs. 4 (a)–(e). As shown in Fig. 4 (a), the strong surface current distributions at U-shape branch, attribute to the length of U-shape branch is 85.6 mm, which corresponds to about 0.25λ at 900 MHz. Figure 4 (b) plots that the surface current at the 1800 MHz is mainly distributed on U-shape branch and coupling branch, which infers that the coupling branch generates a lower-frequency resonant mode around 1800 MHz. In Fig. 4 (c), it can be seen that the surface currents concentrate upon L-shape branch and I-shape driven strip. Figure 4 (d) shows that strong current flows along the I-shape driven strip, which demonstrates that driven strip can provide a 0.25λ resonant mode at about 3350 MHz. Furthermore, the simulated surface current distribution excited at 4800 MHz is illustrated in Fig. 4 (e), in which intense and uniform current distributions can be observed around the rectangular slot. In addition, it can be confirmed from Fig. 4 (e) that the higher-frequency resonant mode at about 4800 MHz is mainly contributed to the rectangular slot of the system ground plane, owing to the path (length 18.4 mm) corresponding to about 0.25λ at 4800 MHz.

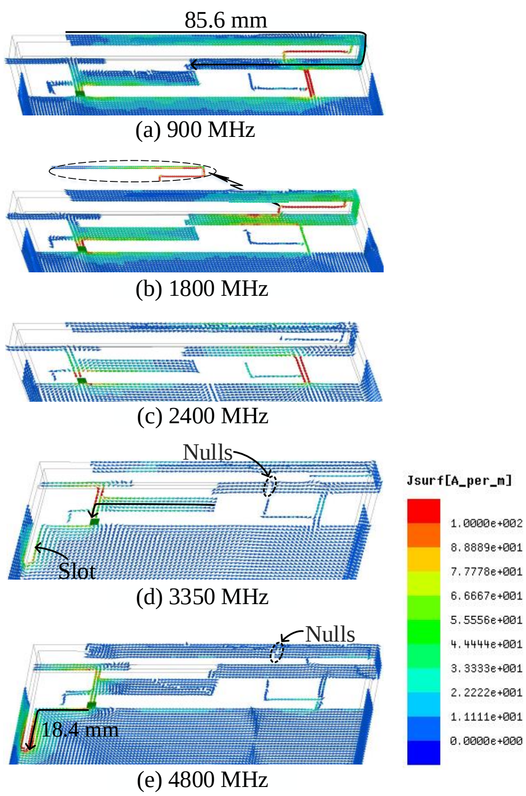

Fig. 4. Simulated surface current distributions at: (a) 900 MHz, (b) 1800 MHz, (c) 2400 MHz, (d) 3350 MHz, and (e) 4800 MHz.

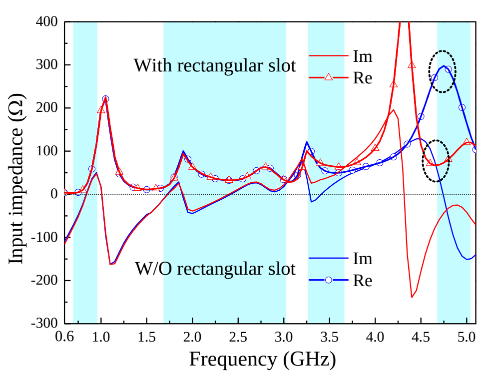

Fig. 5. Effects of the rectangular slot on input impedance.

The rectangular slot has a positive effect on the impedance matching of the proposed antenna in band 4. Figure 5 shows the input impedances with and without the rectangular slot. In band 4, the addition of the rectangular slot decreases the reactance to improve the impedance matching. Therefore, the bandwidth of the band 4 is widely enlarged, covering the 4680–5050 MHz band.

D. Parametric study

In the design of this antenna, changing the length of W_5 and W_1 respectively, the corresponding effects on the resonant mode are depicted at Fig. 6 and Fig. 7. When the length W_5 varies from 17.7 to 22.7 mm, it can be seen from Fig. 6 that the change of antenna's bandwidth is relatively remarkable in band 2 and band 3.

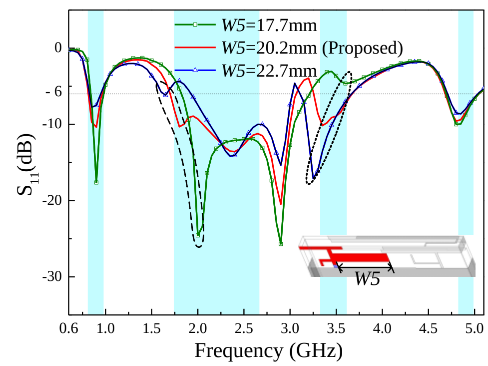

Fig. 6. Simulated S_{11} as a function of the length W_5.

Figure 7 shows the simulated S_{11} as a function of the length W_1 of the U-shape branch. It can be seen from Fig. 7 that when the value of W_1 increases, the antenna bandwidth becomes narrower in band 1. This indicates that the length of the U-shape branch is an important parameter of the designed antenna.

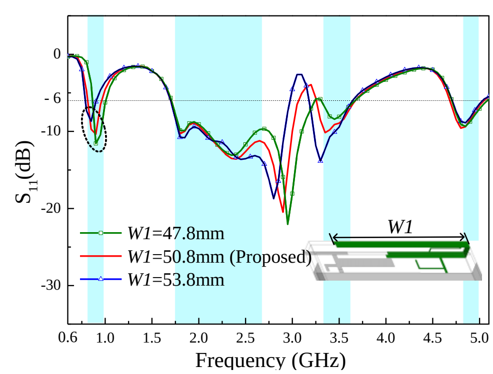

Fig. 7. Simulated S_{11} as a function of the length W_1.

III. EXPERIMENTAL RESULTS AND DISCUSSION

Figure 8 shows the fabricated prototype of the proposed antenna, which is excited by a 50 Ω mini coaxial line. What was used for testing the S-parameters is an Agilent N5247A vector network analyzer. Figure 9 presents the measured results of S_{11}, which is consistent with the simulated results. The measured bandwidths are 822–961 MHz, 1697–3075 MHz, 3280–3835 MHz and 4475–5050 MHz, respectively, and they can cover 824–960 MHz, 1710–2690 MHz, 3300–3600 MHz and 4800–5000 MHz which is widely used as the design specification for 4G/5G mobile antennas.

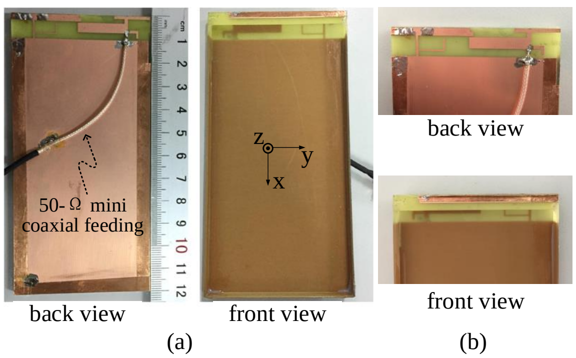

Fig. 8. Photographs of the fabricated antenna. (a) Overall view and (b) enlarged view.

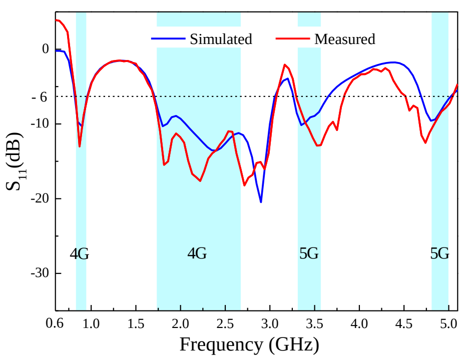

Fig. 9. Comparison between the measured and simulated S_{11} of the proposed antenna.

Figure 10 shows the 2-D radiation patterns of the fabricated prototype at 900, 2400, 3350 and 4800 MHz. As shown in the placement direction of the antenna in Fig. 1, the copol (E_θ) and cross-pol (E_ϕ) in the *xoy*, *yoz* and *zox*-planes are simulated and measured, and it can be concluded from Fig. 10, the E_θ varies smoothly in *yoz*-plane, which is beneficial to actual smartphone applications.

Figure 11 shows the simulated and measured results of the gain and efficiency. It can be concluded from Fig. 11 that the measured results are basically consistent with the simulated results. At the 4G frequency bands, the measured antenna's gain is around 3.2 dBi, and the measured radiation efficiency varies from 51% to 70% measured. In the 5G frequency bands, the measured gain fluctuates from 2.5 dBi to 3.1 dBi. Meanwhile, the efficiency of the proposed antenna fluctuates from 53% to 61%, which can satisfy the requirement of wireless communication for mobile devices. In addition, a comparison between the proposed antenna and the typical reported mobile phones according to the dimensions, frequency bands, bandwidth, and efficiency is shown in Table 2. Thus it can be concluded that the proposed antenna is more suited to 4G/5G metal-rimmed mobile phones.

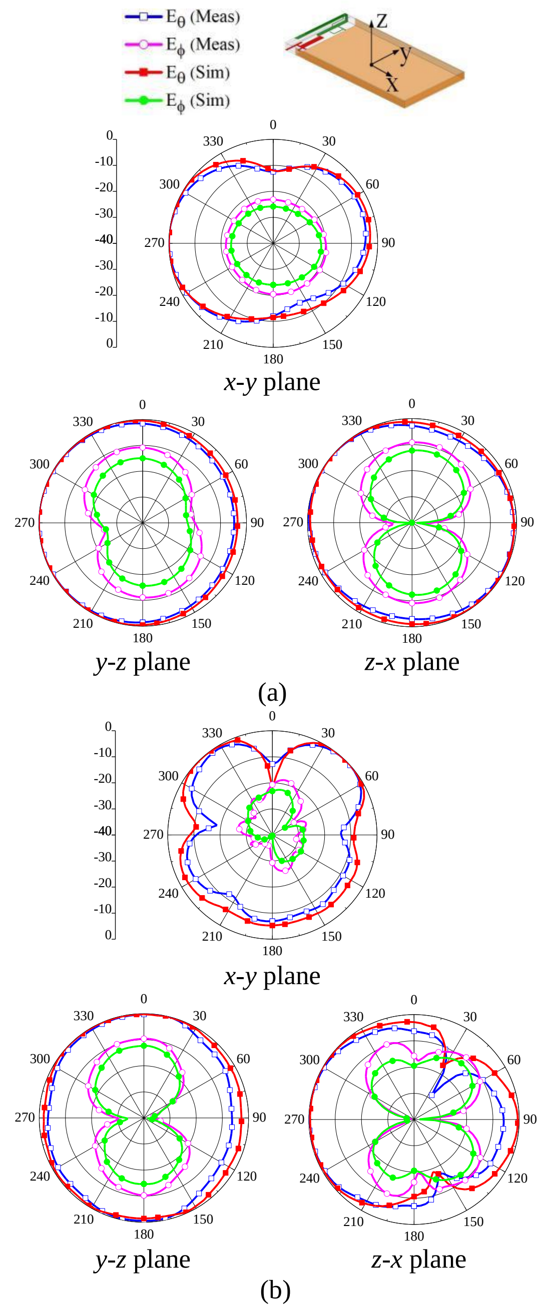

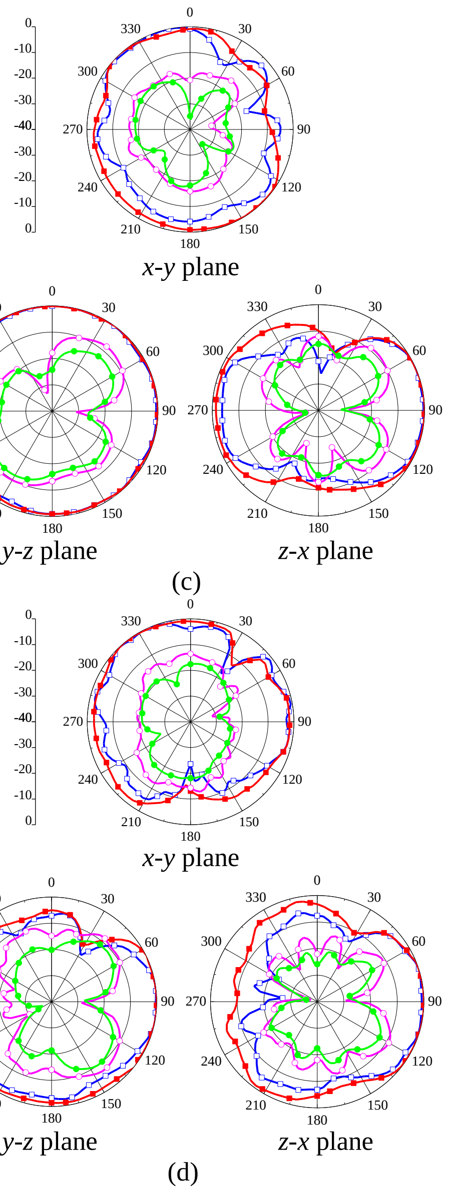

Fig. 10. Simulated and measured 2-D radiation patterns at: (a) 900 MHz, (b) 2400 MHz, (c) 3350 MHz, and (d) 4800 MHz.

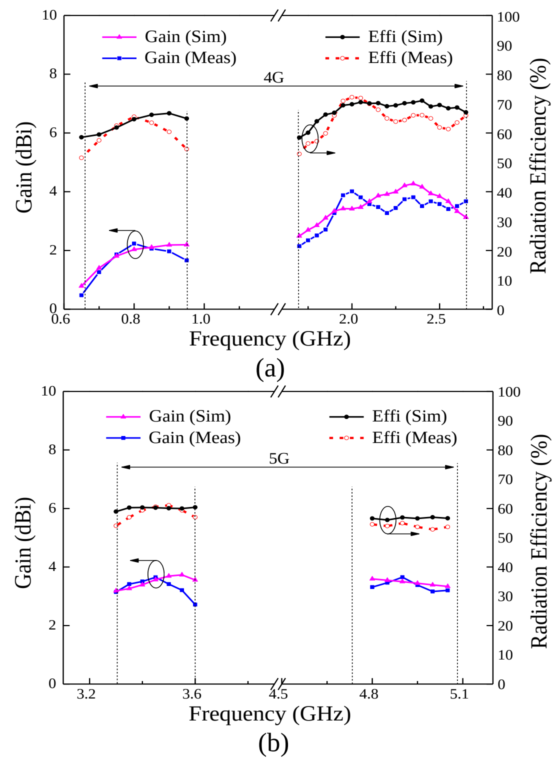

Fig. 11. Simulated and measured gain and efficiency of the proposed antenna: (a) 4G and (b) 5G.

IV. CONCLUSION

A novel multi-mode narrow-frame antenna for 4G/5G metal-rimmed mobile phone is proposed in this paper. The proposed antenna with compact size of 10.4 × 60 mm^2 is integrated on a metal-rimmed mobile phone with size of 120 × 60 × 5 mm^3, which meet the volume requirements of handheld terminals. The bandwidth of the antenna is widened by using meander technologies for the operating band of 822–961 MHz, 1697–3075 MHz which can cover 824–960 MHz, 1710–2690 MHz. The bands of 3280–3835 MHz, 4475–5050 MHz are obtained by slotted loading method which can cover 3300-3600 MHz, 4800-5000 MHz. Therefore, this antenna can satisfy the requirements for smartphone systems without matching circuits or lumped elements.

Table 2: Comparison of proposed antenna and reference antennas

Reference	Dimension (mm^3)	Frequency Band	Bandwidth (MHz)	Gain (dBi)	Efficiency (%)
[1]	72×6.5×5.8	Octa-band	700–1030/1700–2690	1.56/2.38	>46.5/45.5–81.75
[3]	70×9×5	Octa-band	704–960/1700–2830	0.2–2.49/1.18–4.24	44–75/43–76
[7]	71×5×6	Hepta-band	800–1000/1700–2780	–/–	62–85.7/66.9–91
[9]	71.6×10×5	Hepta-band	801–1002/1695–3000	0.7–3.4/2.0–5.0	31–38/42–69
[10]	27×10.8×0.8	Deca-band	685–960/1710–2170/3288–3613	1.4–2.5	40–65/60–92
[16]	120×70×6	Octa-band	675–1050/1600–2800	0–2.1/1.6–3.6	52.7–78.7/45.6–81
[17]	72×8×5	Hepta-band	824–960/1710–2690	0.98–2.1/2.45–5.1	41–48/49–76
[18]	140×70×1	di-band	3300–3600/5150–5925	–/–	51–59/62–80
[20]	100×60×0.5	di-band	2500–2700/3400–3600	–/–	72–88/53–68
Proposed	**60×10.4×5**	**Nona-band**	**822–961/1697–3075/ 3280–3835/4475–5050**	**3.4/2.5–3.1**	**51–70/53–61**

ACKNOWLEDGMENT

This work was supported by the National Natural Science Foundation of China under Grant No. 61172020, the Project of Anhui Local High-level University Construction under Grant No. 2013gx001 and the Key Project of Natural Science Research of Colleges and Universities in Anhui Province under Grant No. KJ2018A0818.

REFERENCES

[1] P. Wang, Y. Shao, D. Huang, and M. A. Basit, "A compact coupled-fed loop antenna for mobile LTE smartphones," *International Journal of Antennas and Propagation*, vol. 2018, Article ID 8426574, 8 pages, 2018.

[2] Y. Wang and Z. W. Du, "Wideband monopole antenna with less nonground portion for octa-band WWAN/LTE mobile phones," *IEEE Transactions on Antennas and Propagation*, vol. 64, no. 1, pp. 383-388, 2016.

[3] P. Y. Qiu and Q. Y. Feng, "Low-profile compact antenna for octa-band metal-rimmed mobile phone applications," *IEEE Transactions on Antennas and Propagation*, vol. 68, no. 1, pp. 54-61, Jan. 2020.

[4] Q. G. Chen, H. W. Lin, and J. P. Wang, L. Ge, Y. Li, T. Pei and C. Y. D. Sim, "Single ring slot-based antennas for metal-rimmed 4G/5G smartphones," *IEEE Transactions on Antennas and Propagation*, vol. 67, no. 3, pp. 1476-1487, Mar. 2019.

[5] K. L. Wong and C. Tsai, "Half-loop frame antenna for the LTE metal-casing tablet device," *IEEE Transactions on Antennas and Propagation*, vol. 65, no. 1, pp. 71-81, Jan. 2017.

[6] J. W. Lian, Y. L. Ban, Y. L. Yang, L. W. Zhang, C. Y. D. Sim, and K. Kang, "Hybrid multi-mode narrow-frame antenna for WWAN/LTE metal-rimmed smartphone applications," *IEEE Access*, no. 4, pp. 3991-3998, Aug. 2017.

[7] Y. Liu, J. K. Zhang, A. D. Ren, H. Wang, and C. Y. D. Sim, "TCM-based hepta-band antenna with small clearance for metal-rimmed mobile phone applications," *IEEE Antennas and Wireless Propagation Letters*, vol. 18, no. 4, pp. 714-721, Apr. 2019 .

[8] K. L. Wong, C. Tsai, and J. Y. Lu, "Two asymmetrically mirrored gap-coupled loop antennas as a compact building block for eight-antenna MIMO array in the future smartphone," *IEEE Transactions on Antennas and Propagation*, vol. 65, no. 4, pp. 1765-1778, 2017.

[9] L. W. Zhang, Y. L. Ban, and C. Y. D. Sim, J. Guo, and Z.-F. Yu, "Parallel dual-loop antenna for WWAN/LTE metal-rimmed smartphone," *IEEE Transactions on Antennas and Propagation*, vol. 66, no. 3, pp. 1217-1226, Mar. 2018.

[10] M. Yang, Y. F. Sun and F. Li, "A compact wideband printed antenna for 4G/5G/WLAN wireless applications," *International Journal of Antennas and Propagation*, ID: 3209840, 2019.

[11] Cursor, "New antenna technology for extremely fast 5G and 6G," May 11, 2019. [Online]. Available: https://www.cursor.tue.nl/en/news/2019/november/week-1/new-antenna-technology-for-extremely-fast-5g-and-6g/

[12] J. Happich, "5G-ready MIMO 4×4 antenna for indoor applications," Nov. 27, 2019. [Online]. Available: https://www.eenewseurope.com/news/5g-ready-mimo-4x4-antenna-indoor-applications

[13] K. L. Wong and Y. C. Chen, "Small-size hybrid loop/open-slot antenna for the LTE smartphone," *IEEE Transactions on Antennas and Propagation*, vol. 63, no. 12, pp. 5837-5841, Dec. 2015.

[14] K. L. Wong and C. Tsai, "IFA-based metal-frame antenna without ground clearance for the LTE/ WWAN operation in the metal-casing tablet computer," *IEEE Transactions on Antennas and Propagation*, vol. 64, no. 1, pp. 53-60, 2016.

[15] J. Choi, W. Hwang, C. You, B. Jung, and W. Hong, "Four-element reconfigurable coupled loop MIMO antenna featuring LTE full-band operation for metallic-rimmed smartphone," *IEEE Transactions on Antennas and Propagation*, vol. 67, no. 1, pp. 99-107, 2019.

[16] D. W. Huang and Z. W. Du, "Eight-band antenna with a small ground clearance for LTE metal frame mobile phone applications," *IEEE Antennas and Wireless Propagation Letters*, vol. 17, no. 1, pp. 34-37, Jan. 2018.

[17] Z. Q. Xu, Q. Q. Zhou, Y. L. Ban, and S. S. Ang, "Hepta-band coupled-fed loop antenna for LTE/WWAN unbroken metal-rimmed smartphone applications," *IEEE Antennas and Wireless Propagation Letters*, vol. 17, no. 2, pp. 311-314, Feb. 2018.

[18] J. X. Li, X. K. Zhang, Z. Wang, X. Chen, J. Chen, Y. Li, and A. Zhang, "Dual-band eight-antenna array design for MIMO applications in 5G mobile terminals," *IEEE Access*, no. 7, pp. 71636-71644, 2019.

[19] Y. L. Ban, C. Li, C. Y. D. Sim, G. Wu, and K. L. Wong, "4G/5G multiple antennas for future multi-mode smartphone applications," *IEEE Access*, no. 4, pp. 2981-2988, July 2016.

[20] F. Liu, J. Y. Guo, L. Y. Zhao, G. L. Huang. Y. S. Li, and Y. Z. Yin, "Dual-band metasurface-based decoupling method for two closely packed dual-band antennas," *IEEE Transactions on Antennas and Propagation*, vol. 68, no. 1, pp. 552-557, 2020.

[21] K. Yu, Y. S. Li, and X. G. Liu, "Mutual coupling reduction of a MIMO antenna array using 3-D novel meta-material structures," *Applied Computational Electromagnetics Society Journal*, vol. 33, no. 7,

pp. 758-763, 2018.

[22] S. Y. Luo, Y. S. Li, Y. F. Xia, and L. Zhang, "A low mutual coupling antenna array with gain enhancement using metamaterial loading and neutralization line structure," *Applied Computational Electromagnetics Society Journal*, vol. 34, no. 3, pp. 411-418, 2019.

[23] J. F. Jiang, Y. F. Xia, and Y. S. Li, "High isolated X-band MIMO array using novel wheel-like metamaterial decoupling structure," *Applied Computational Electromagnetics Society Journal*, vol. 34, no. 12, pp. 1829-1836, 2019.

Ming Yang was born in 1982. He received the B.S. and the M.S degrees from Huaibei Normal University and Anhui University in 2005 and 2010, respectively, and the Ph.D. degree in Electromagnetic Field and Microwave Technology with Anhui University in 2019.

His research interest includes antenna theory and antenna design.

Yu-fa Sun was born in 1966. He received the B.S. and M.S. degrees from Shandong University in 1988 and 1991, respectively, and the Ph.D. degree in Electromagnetic Field and Microwave Technology from the University of Science and Technology of China in 2001.

Since 1991, he has been a faculty member in the Department of Electronic Engineering, Anhui University, China, where he is currently a Full Professor. He was a Visiting Scholar at the Wireless Communication Center at the City University of Hong Kong from February 2002 to January 2003. His research interests include computational electromagnetics and antenna theory and technology. He has authored or coauthored more than 150 journal and conference papers.